TÜBİTAK

Turkish Journal of Chemistry

http://journals.tubitak.gov.tr/chem/

Research Article

Turk J Chem
(2016) 40: 565 – 575

doi:10.3906/kim-1507-7

Preparation, characterization, and adsorption studies of core@shell SiO_2@CeO_2 nanoparticles: a new candidate to remove Hg(II) from aqueous solutions

Ali İmran VAİZOĞULLAR[1,*], Ahmet BALCI[2],İbrahim KULA[2], Mehmet UĞURLU[2]

[1]Medical Services and Techniques Department, Vocational School of Health Services, Muğla Sıtkı Koçman University, Muğla, Turkey

[2]Department of Chemistry, Faculty of Science, Muğla Sıtkı Koçman University, Muğla, Turkey

Received: 03.07.2015 • **Accepted/Published Online:** 07.12.2015 • **Final Version:** 21.06.2016

Abstract: SiO_2 supported core@shell nanoparticles (CSNs) have recently attracted great attention due to their unique, tunable, optical, photocatalytic, and higher adsorption properties. In this study, SiO_2@CeO_2 CSNs were synthesized using a chemical precipitation technique and characterized by Fourier transform infrared (FT-IR), X-ray diffraction (XRD), scanning electron microscope (SEM), and transmission electron microscope (TEM) analysis. XRD analysis showed that SiO_2 particles were the core while CeO_2 particles were the shell. It was seen as a new band at 961 cm^{-1} of the oxygen bridge between Si and Ce atoms from FT-IR results; SiO_2 and CSNs were spherical (0.5–0.6 μm) from SEM and TEM analyses. Different parameters such as contact time, initial concentration, pH, and temperature were investigated. The optimum conditions for temperature, pH, and contact time were 25 °C, 8.0, and 60 min, respectively. In addition, the equilibrium adsorption data were interpreted using Langmuir and Freundlich models to describe the uptake of Hg(II). The Freundlich isotherm model (R^2: 0.99) fit better than Langmuir and the q_{max} value was 153.8 μg g^{-1} at various concentrations (0.1–1 mg L^{-1}). The thermodynamic parameters were also calculated and, from these results, it can be shown that our synthesized particles can be used in water purification systems to remove Hg(II).

Key words: SiO_2/CeO_2, mercury, heavy toxic metal, core@shell, adsorption

1. Introduction

Mercury is a highly toxic and accumulative metal and its compounds, especially methyl mercury, are neurotoxins that cause blockages of the enzyme sites and interfere with protein synthesis. The fate of inorganic mercury ions in nature is to turn into methyl mercury, owing to the aerobic action of microorganisms. The main sources of mercury ions in aquatic ecosystems are divergent: chlor-alkali oil refineries, wastewater, power generation plants, paper and pulp manufacturing, rubber processing, and the fertilizer industry.[1] The tolerance limit for Hg(II) discharged into inland surface waters is 10 μg L^{-1}, while in drinking water it is 1 μg L^{-1}.[2] Mercury toxicity is highly dependent upon its oxidation state.[3] Hg(II) is very reactive and binds to the amino acid cysteine proteins; thus this form is more toxic.

Physical and chemical processes to remove mercury from wastewater at high concentrations have been studied extensively. Some of these processes are adsorption, chemical precipitation,[4] coagulation,[5] flotation,

*Correspondence: vaizogullar@yahoo.com

and electrochemical methods.[6] Adsorption can be seen as an efficient and economical method for the removal of mercury and, from time to time, it may be needed for different adsorbent materials to remove it at ppb level. In the present study, the aim was to synthesize CSNs as adsorbent material. In the literature, it was reported that CSNs have been prepared by various synthetic procedures,[7] e.g., sol-gel,[8] microemulsion,[9] and thermal reduction.[10] In addition, cerium dioxide (CeO_2) based micro-materials have been applied as catalysts, catalyst supports, cosmetics, ceramics, O_2 sensors, solid oxide fuel cells, and fluorescent materials.[11] In this context, we synthesized a new material based on CSNs; then the adsorption of Hg(II) ions was carried out by using this material in batches. The parameters affecting the adsorption of Hg(II) (time, pH, initial concentration and temperature, adsorbent dosage) were investigated. The data thus obtained were fitted to the Freundlich and Langmuir isotherm models and the thermodynamic properties, including enthalpy, entropy, and Gibbs free energy, were determined from the experimental results.

2. Results and discussion

2.1. Characterization of CeO_2 and CSNs

2.1.1. XRD analysis

Figure 1 shows the XRD spectrum of CeO_2 and CSNs. When XRD results belonging to these samples were evaluated, both diffractograms showed four characteristic peaks at 28.43°, 32.92°, 47.38°, and 56.27° at 2θ degrees (Figures 1a and 1b). These peaks can be attributed to the (111), (200), (220), and (311) planes of the cubic fluorite structure of CeO_2 (JCPDS 34-394). It means that the shell area of CSNs is composed of CeO_2.

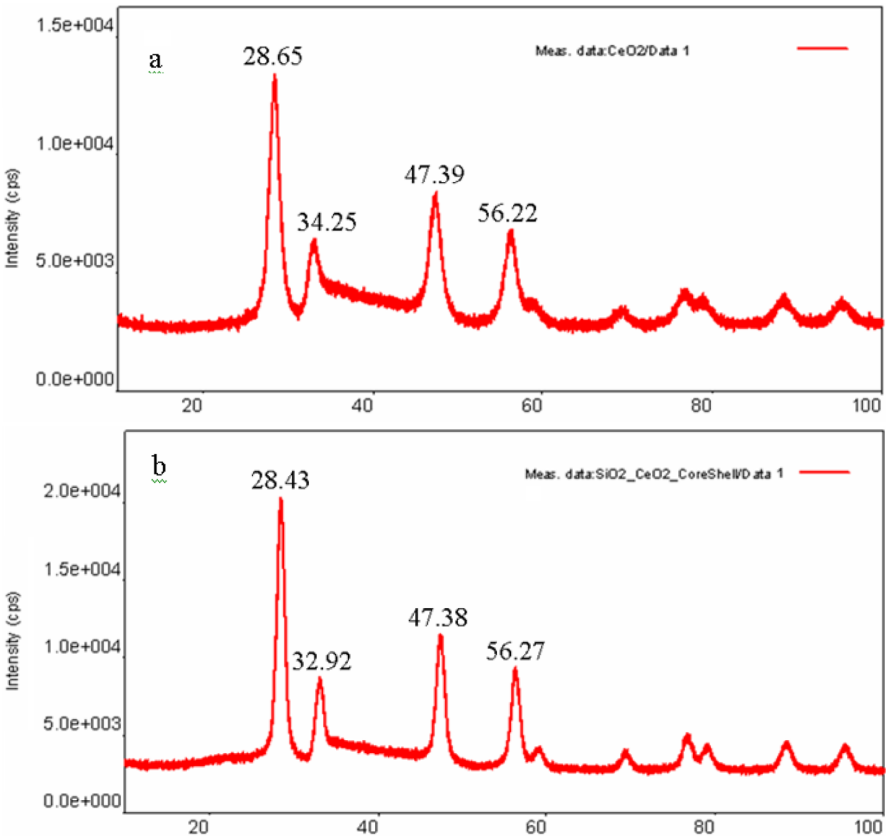

Figure 1. XRD patterns of CeO_2 particles (a) and SiO_2/CeO_2 particles (b).

When Figure 1b was evaluated, a tiny broad peak was observed at 20–22.5° belonging to SiO_2 at the same time. It is estimated that the core area of CSNs is composed of SiO_2 because the new phase was not observed, indicating the individual phases of SiO_2 and CeO_2 considering previous similar studies.[12]

2.1.2. FT-IR analysis

The FT-IR spectra of SiO_2 microparticle and CSNs are shown in Figures 2a and 2b, respectively. These spectra clearly show a broad band at 3404 and 3423 cm^{-1} that belongs to O–H stretching of water for both particles. The band at 1554 cm^{-1} is attributed to the bending vibrations of associated water (Figure 2b).[13] Si–O–Si asymmetric stretching of SiO_2 particles was observed at 1105 cm^{-1} for SiO_2 microparticle (Figure 2a). After coating SiO_2 particles with CeO_2, it was observed that the peak at 1104 cm^{-1} reflected a shift to 1054 cm^{-1}. This is because CeO_2 has created effective repression on SiO_2 (Figure 2b). The same result was reported by Song et al. during the synthesis of SiO_2 microparticles and SiO_2@CeO_2 CSNs.[13] In addition, one can easily observe the extra bands at 961 cm^{-1} and 411 cm^{-1} (Figure 2b). The band at 961 cm^{-1} belongs to Ce–O–Si stretching, while the band at 411 cm^{-1} is attributed to Ce–O stretching. Another band at 1377 cm^{-1} is attributed to the N–O stretching from Ce $(NO_3)_3.6H_2O$ in particles (Figure 2b).[13]

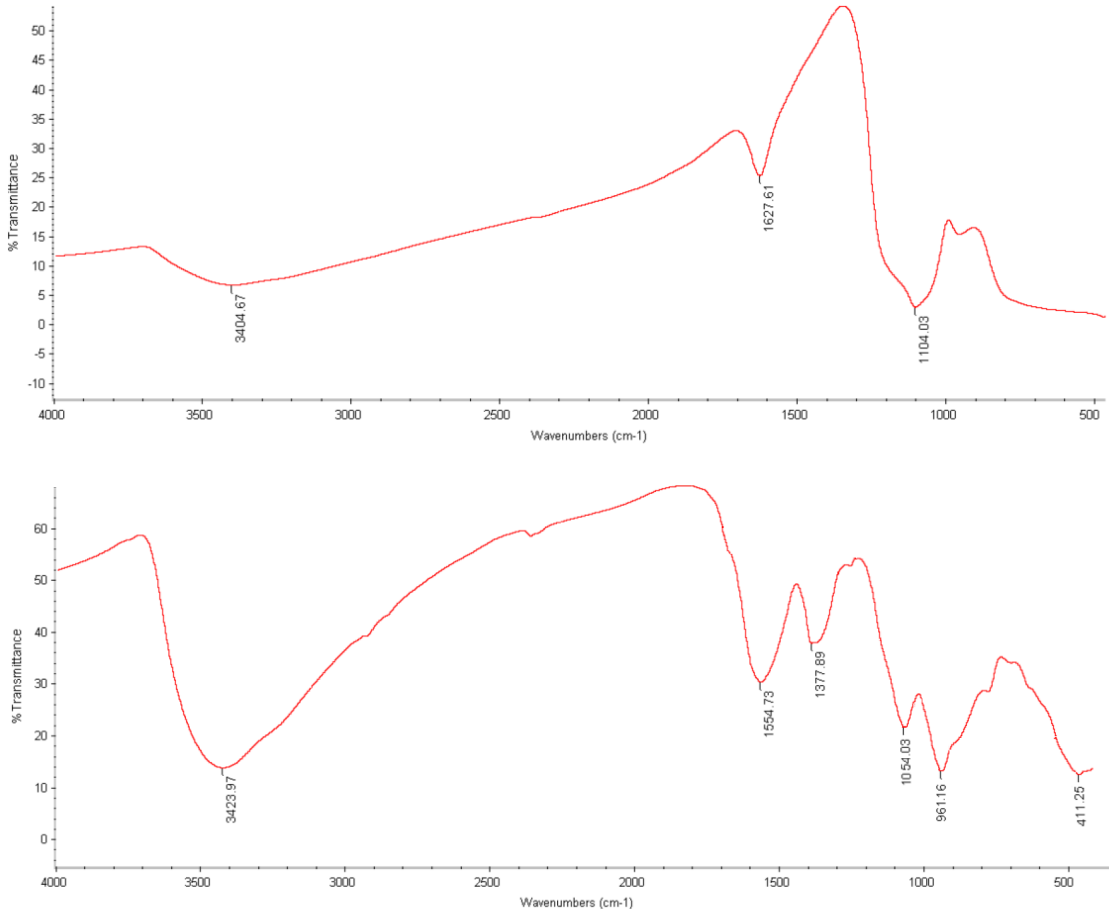

Figure 2. IR spectra of SiO_2 particles (a) SiO_2/CeO_2 particles (b).

2.1.3. SEM and EDAX analyses

SEM analysis can provide information about the size and shape of the particles. Figures 3 and 4 show the SEM images of SiO_2 and SiO_2@CeO_2 CSNs. As seen from Figure 3, while SiO_2 particles were smooth, spherical, and very uniform in structure, agglomeration was seen in the SEM image belonging to CSNs because of the impregnation method (Figures 4a–4d). It was seen that the particle size of CSNs increased and a prominent

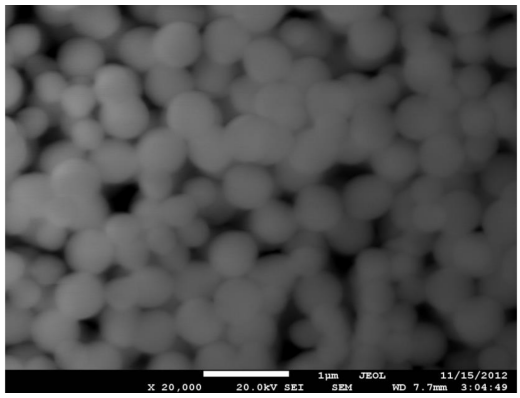

Figure 3. SEM images of SiO_2 particles.

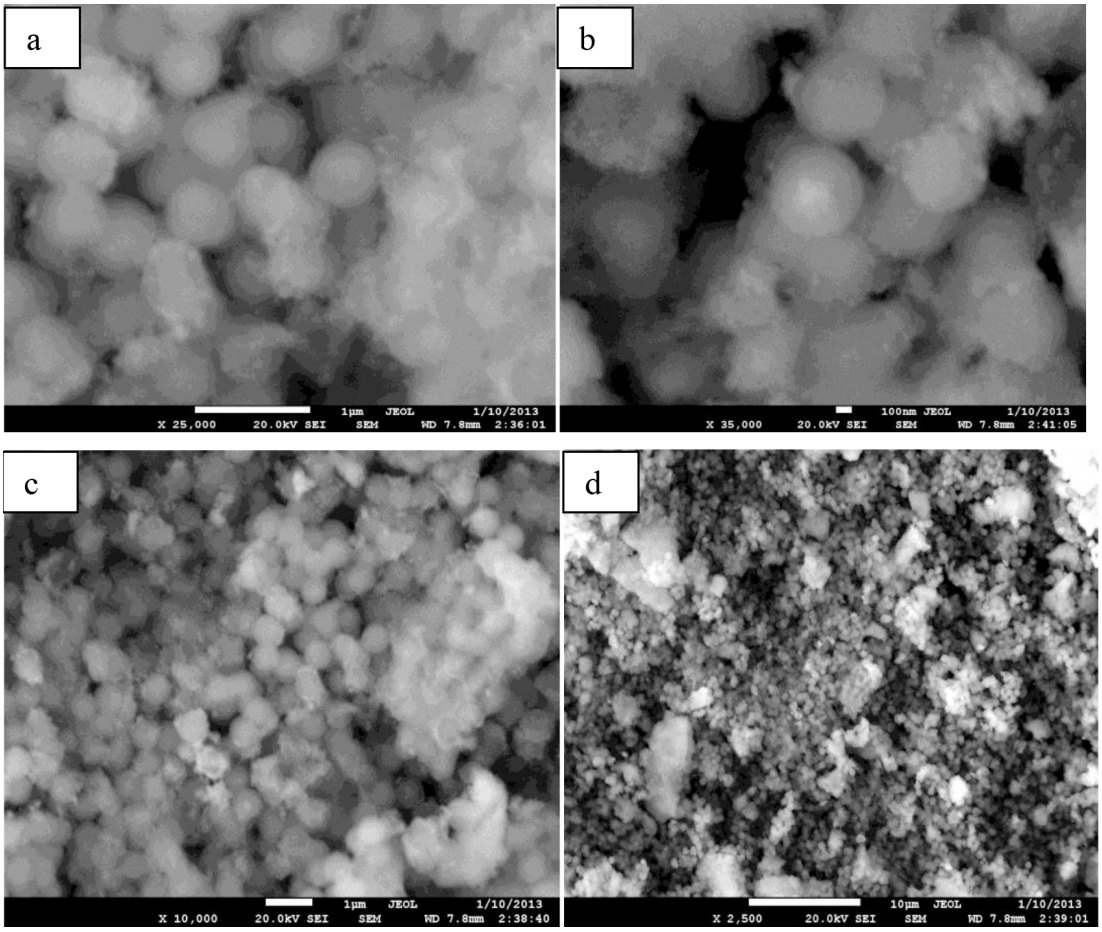

Figure 4. SEM images of SiO_2/CeO_2 core shell particles (a, b, c, d).

and nonuniform layer of CeO_2 could be observed. The average diameter of CSNs was observed at 600–700 nm approximately from Figure 4a. In addition, the EDAX spectrum confirmed the presence of CeO_2 in CSNs qualitatively and EDAX analysis along the cursor crossing showed that Ce was located at the end and Si was first. It could be said CeO_2 was the shell and SiO_2 was the core (Figure 5).

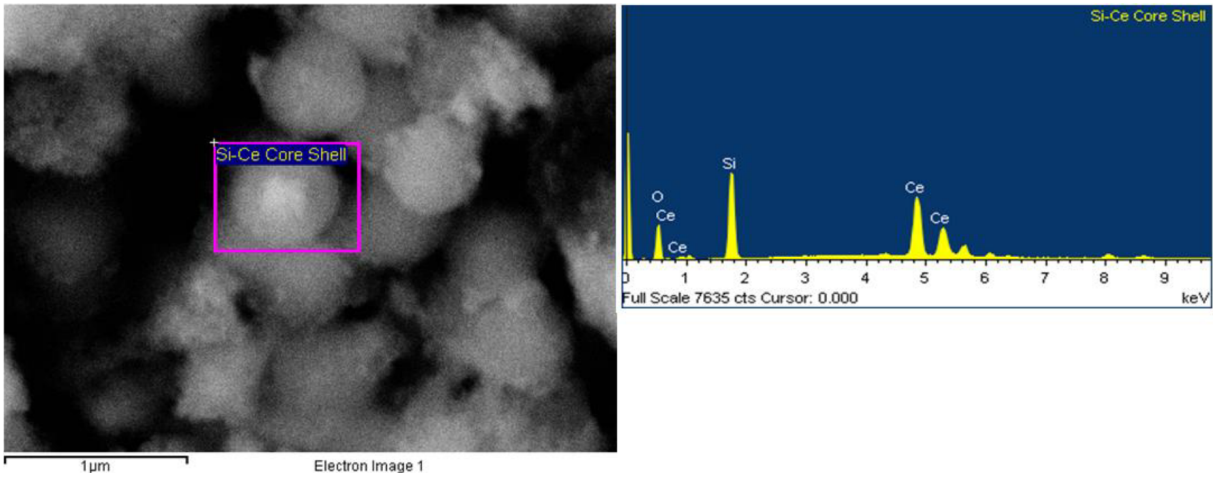

Figure 5. EDAX analysis of SiO_2/CeO_2 core shell particles.

2.1.4. Transmission electron microscopy (TEM) analysis

TEM images of the nanocomposites can give information about the morphology of composite particles. In this study, TEM images of CSNs are shown in Figure 6. From Figure 6, it appeared that the particle size increased after coating. In addition, it was observed in the form of aggregates heterogeneously on SiO_2 surface and CSNs are clearly visible on the surface of SiO_2 (Figures 6a–6c). The wall thickness of SiO_2 particles was about 35–40 nm (Figure 6a).

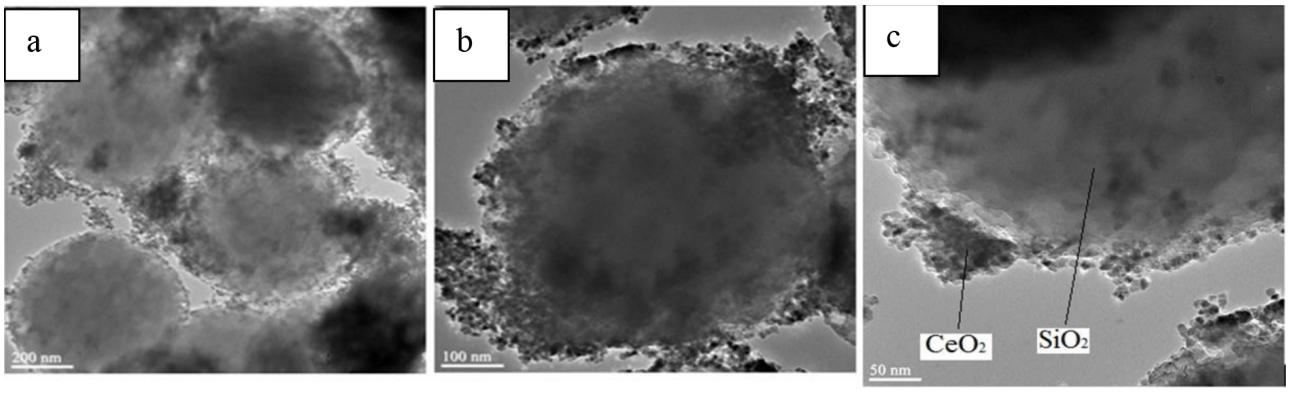

Figure 6. TEM analysis of SiO_2/CeO_2 particles (a, b, c).

3. Effect of parameters in adsorption experiments

3.1. Effect of contact time and pH

The removal of metal ions from aqueous solutions by adsorption is highly dependent on the pH of the solution, which affects the surface charge of the adsorbent and the degree of ionization and speciation of the adsorbate.

Most research has been conducted on heavy metal sorption, which indicated that the decrease in ion sorption at acidic pH may be due to the increase in competition with protons for active sites. However, at alkaline pH values, other effects may arise from some processes, such as the predominant presence of hydrated species of heavy metals, changes in surface charge, and precipitation of the appropriate salt.[14–16] To verify the effect of pH on Hg(II) adsorption using the core shell particles, experiments were conducted modifying pH from 2 to 10 (Figures 7 and 8). As seen from Figure 7, the highest adsorption occurred after 60 min and reached equilibrium. Adsorption of Hg(II) increased with the increase in pH but a decrease in Hg adsorption after this pH value was observed (Figure 8). This can be explained by the supramolecular interactions between the surface of CSNs and Hg(II).

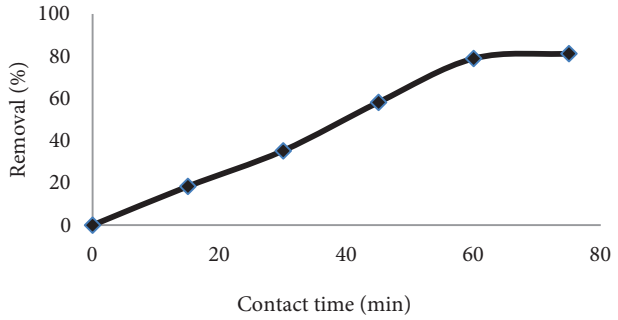

Figure 7. Effect of contact time for adsorption of Hg(II) by SiO_2/CeO_2 particles (Hg(II) concentration = 1 mg L^{-1}, solid/liquid: 0.05 g/25 mL, pH 8, and 25 °C).

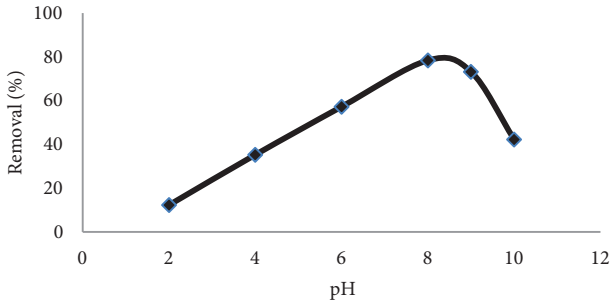

Figure 8. The effect of pH on the removal of Hg(II) for adsorption of Hg(II) by SiO_2/CeO_2 particles (Hg(II) concentration = 1 mg L^{-1}, solid/liquid: 0.05 g/25 mL, contact time 60 min, and 25 °C).

Song et al. also reported that the surface of CSNs is negatively charged under basic conditions.[13] Therefore, the electrostatic attraction provides a supramolecular interaction between the surface of CSNs and positively charged Hg(II). Under acidic conditions, the supramolecular interactions will vanish as positively charged Hg(II) will not adsorb on the surface of the same charged particles. Therefore, at high pH values, the degree of surface protonation gradually decreases and the removal capacity of Hg(II) from the solution increases.[17,18] In addition, the removal percentage of Hg(II) from solutions after pH 8 decreased sharply because of excessive OH^- ions that caused the occurrence of metal hydroxide species such as soluble $Hg(OH)^+$ or insoluble of $Hg(OH)_2$.[19]

The probable surface exchange of CSNs in acidic and alkaline conditions is shown in the following equation:

$$\underset{\text{Positive charged surface in acidic medium}}{\text{SiCe}} \xleftrightarrow{H^+} \text{SiCe-}H^+ \xleftrightarrow{OH^-} \underset{\text{Negative charged surface in pH 6–8}}{\text{SiCeOH-Hg(II)}} \xleftrightarrow{OH^-} \underset{\text{Hydrolyze precipitation of Hg(II) at pH} > 8}{Hg(OH)_2 + \text{SiCe}}$$

3.2. Effect of temperature

The effect of temperature was investigated at various temperatures and plotted in Figure 9. The adsorption efficiency of particles was inversely proportional to the temperature. This means that the adsorption was exothermic.[20] This result was attributed to the increased tendency of Hg(II) to become distant from the particle surface when the solution temperature increased.[21]

This can be explained by the adsorption and diffusion process being inversely proportional. The adsorption capacity decreases with increasing temperature. This indicates that the adsorption process is more predominant than the diffusion process. This also suggests that CSNs were regular microspheres. Because the irregular structure provides pore obstacles, the Hg(II) ions could not activate in the pores easily, resulting in diffusion rather than adsorption.[21]

3.3. Effect of initial concentration

When the effect of initial concentration was examined at different concentrations, it was observed that adsorption was increased by increasing the initial concentration initially (Figure 10), and was then held constant as the adsorption probability is higher at higher concentrations. In the present study, we found that q_e values at initial concentration of 0.1 mg L^{-1} and 1 mg L^{-1} were 19.31 μg g^{-1} and 135.36 μg g^{-1}, respectively. It can be concluded that CSNs surface adsorbed most of the Hg(II) ions at low initial concentrations. When the initial concentrations of Hg(II) increased, the ratio of active sites of particle surface to initial Hg(II) concentration decreased and resulted in a reduced Hg(II) percentage.[22]

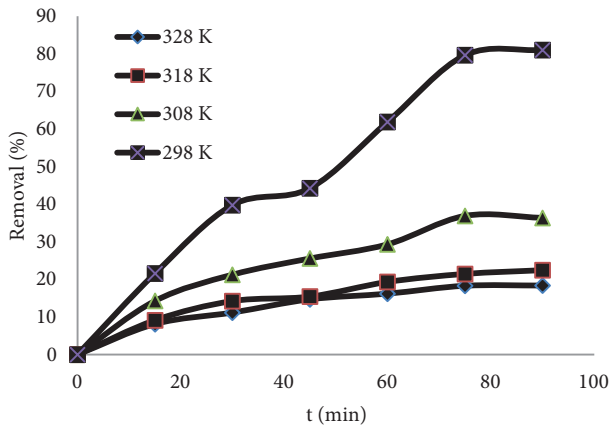

Figure 9. Effect of temperature on adsorption of Hg (II) over SiO_2/CeO_2 particles; (Hg(II) concentration = 1 mg L^{-1}, amount of adsorbent = 0.05 g, volume of solution = 25).

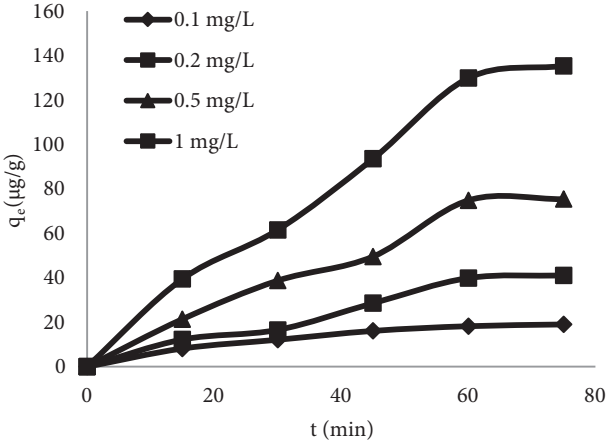

Figure 10. Effect of initial concentration on adsorption of Hg(II) over SiO_2/CeO_2 particles (amount of adsorbent = 0.05 g volume of solution = 25 mL, pH 8, time = 60).

3.4. Adsorption isotherms

Adsorption of Hg(II) surface CSNs was studied at different concentrations with different initial concentrations. Langmuir (Figure 11) and Freundlich (Figure 12) adsorption isotherms are most commonly used to express adsorption studies. The Langmuir isotherm is generally used to represent the monolayer adsorption of adsorbate onto adsorbent surfaces. This monolayer adsorption can be chemi- or physisorption but should reduce the desorption process and not react with each other.[23] The Langmuir adsorption model is shown in the following equations:

$$q_e = \frac{q_e K C_e}{1 + K C_e}$$

$$\frac{C_e}{q_e} = \frac{1}{q_m K} + \frac{C_e}{q_m},$$

where q_e is the equilibrium concentration on adsorbent (μg g^{-1}), q_m is the maximum adsorption capacity (μg g^{-1}), K the affinity constant (L μg^{-1}), and C_e is the solution concentration at equilibrium (μg L^{-1}). K and q_m can be determined from a plot of C_e/q_e versus C_e (Figure 11).

The Freundlich adsorption model is an empirical equation based on multilayer adsorption and describes multilayer adsorption on heterogeneous surfaces. The most common equations of Freundlich adsorption isotherms are as follows:[24]

$$q_e = K_F C_e^{\frac{1}{n}}$$

$$lnq_e = lnK_F + \frac{1}{n} lnC_e$$

K_F and n are Freundlich constants and indicate the adsorption capacity and adsorption intensity, respectively.

Figure 12 shows the Freundlich adsorption isotherm where $\ln q_e$ is plotted against $\ln C_e$. *1/n* and K_F were calculated using the slope and intercept, respectively. The constant n gives an idea of the multilayer adsorption capacity. High n values therefore indicate a relatively uniform adsorbent surface, whereas low values mean high adsorption at lower solution concentrations. Furthermore, a low n value indicates the existence of a high proportion of high-energy active sites.[25] The values of *1/n* were between 0 and 1, which indicated that adsorption was favorable.

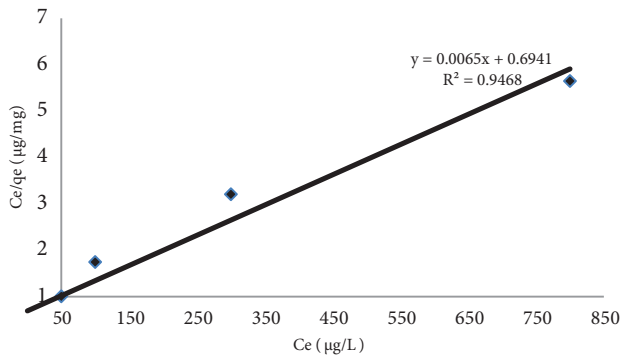

Figure 11. Langmuir adsorption isotherms of Hg(II) ions on SiO_2/CeO_2 particles.

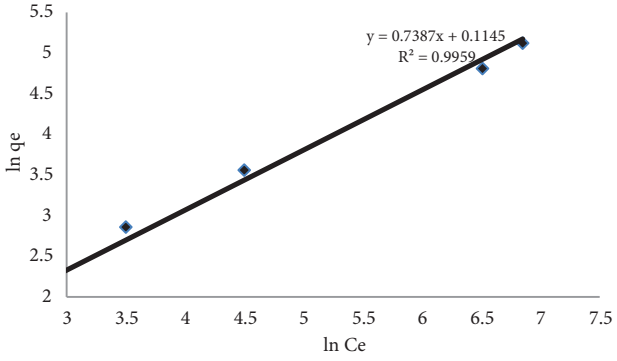

Figure 12. Freundlich adsorption isotherms of Hg(II) ions adsorption on SiO_2/CeO_2 particles.

According to Figures 11 and 12, Freundlich isotherms better explain the adsorption of Hg(II) than Langmuir isotherms, as reflected in the correlation coefficient (Table 1). The results were expected as the Freundlich isotherm is an empirical equation and is satisfactory at low concentrations of adsorbate.[26]

Table 1. Freundlich and Langmuir parameters for adsorption of Hg(II) ions on SiO_2/CeO_2 particles.

Adsorbent	Freundlich isotherm			Langmuir isotherm		
SiO_2/CeO_2	K_F (L μg^{-1})	1/n	R^2	q_{max} (μg g^{-1})	K (10^{-3})	R^2
	1.12	0.74	0.99	153.8	9.37	0.94

3.5. Thermodynamic parameters

The thermodynamic parameters, e.g., Gibbs free energy (ΔG°), enthalpy (ΔH°), and entropy (ΔS°) of Hg(II) removal from aqueous solution were measured using

$$\Delta G^\circ = RTlnK_L = RTln\frac{C_a}{C_e}$$

The enthalpy and entropy values were determined from the plot of lnK_L versus 1/T as shown in Figure 13. Slope is positive when the adsorption is exothermic and temperature is increasing. ΔG°, ΔH°, and ΔS° values are negative at 298 K (Table 2). ΔG° becomes positive when the temperature is increased. Thus, the adsorption process is favorable at low temperatures. The negative Gibbs free energy values indicate the applicability of the process and the spontaneous nature of adsorption. The percentage of adsorption decreased with temperature and the negative ΔH° values indicate the exothermic character of the process.[27,28]

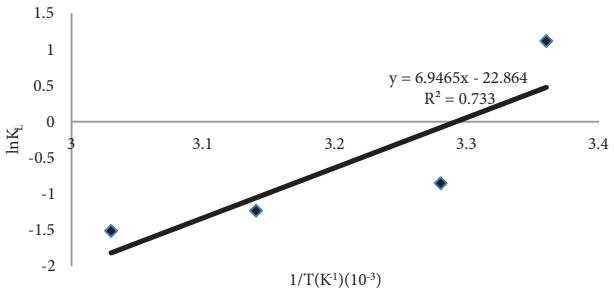

Figure 13. Thermodynamic parameters for adsorption of Hg(II) onto SiO_2/CeO_2 particles.

Table 2. Thermodynamic parameters for adsorption of Hg(II) and SiO_2/CeO_2 particles.

T (K)	ΔH° (kJ/mol)	ΔS° (J/mol K)	ΔG° (kJ/mol)
298	−57.7	−190.1	−1.05
308			0.85
318			2.75
328			4.65

4. Experimental

4.1. Chemicals

Tetraethylorthosilicate (TEOS), concentrated ammonia ($NH_3 \cdot H_2O$), ammonium carbonate monohydrate ($(NH_4)_2CO_3 \cdot H_2O$), cerium nitrate hexahydrate ($Ce(NO_3)_3 \cdot 6H_2O$), absolute ethanol (C_2H_5OH), sodium hydroxide (NaOH), and CTAB were purchased from Sigma Chemicals (USA). Nitrate monohydrate Hg $(NO_3)_2$ was from Merck and all the chemicals were of analytical grade. A stock solution (1000 mg L^{-1}) of Hg(II) was prepared by dissolving the required amounts of Hg $(NO_3)_2$ in distilled/deionized water.

4.2. Characterization

The crystals were examined by XRD (Rigaku Dmax 350) using copper Kα radiation (λ= 0.154056 nm). The FT-IR analysis of precursor was carried out employing the FT-IR measurement system, Thermo-Scientific, (Nicolet IS10-ATR). Microstructure and the shapes of CSNs were investigated by SEM (JEOL JSM-7600F) and

TEM (JEOL JEM 2100F HRTEM). Elemental analysis was performed by (JEOL JSM-7600F) EDAX analyzer with SEM measurement.

4.3. Preparation of materials

4.3.1. 4Preparation of SiO_2

SiO_2 particles were synthesized by the sol-gel method. First 50 mL of NH_3 solution and 25 mL of absolute ethanol were mixed into 50 mL of distilled water, followed by the drop-wise addition of 20 mL of TEOS and stirring for 4 h. Silica particles (SiO_2) were obtained that were washed three times with water and oven dried at 80 °C. After being dried, the particles were calcined for 3 h at 600 °C.

4.3.2. Preparation of SiO_2@/CeO_2 CSNs

First 0.2 g of CTAB was dissolved in 100 mL of water, and to that mixture 1.0 g of SiO_2 cores and 1.5 g of $Ce(NO_3)_3{\cdot}6H_2O$ were added. The pH of the mixture was adjusted to 10 by using 0.01 mol L^{-1} NaOH solution. The reaction mixture was stirred for 4 h and aged for 2 h. The obtained CSNs were filtered, washed with deionized water, oven dried at 80 °C for almost 12 h, and calcined at 400 °C for 3 h.

4.3.3. Metal adsorption experiments

Hg(II) removal was performed in a beaker containing 25 mL of (1 mg L^{-1}) Hg $(NO_3)_2$ solution. The effects of pH, contact time, concentration, and temperature were studied during all adsorption experiments. The amount of the adsorbent was held constant at 0.05 g in 25 mL of 1 mg L^{-1} aqueous solution of Hg(II). Adsorption isotherms were measured at optimum conditions at a contact time of 60 min at pH 8.0 and 25 °C on surface CSNs. The equilibrium adsorption capacities of the adsorbents were calculated using the following equation:

$$q_e = \frac{(C_o - C_e) \cdot V}{m}$$

where q_e is the adsorption capacity (in μg Hg(II) per g of adsorbent), C_o is the initial concentration of Hg(II) (μg L^{-1}), C_e is the equilibrium concentration of Hg(II) (μg L^{-1}), V is the volume of Hg(II) solution, and m is amount of adsorbent. Removal amount of Hg(II) as a percentage was calculated using

$$\text{Removal } (\%) = \frac{(C_o\ C_e)}{C_o} \times 100$$

4.3.4. Determination of Hg(II)

The concentration of mercury was measured by the cold vapor atomic absorption spectrometry (CV-AAS) technique. CV-AAS has become the most widely used technique for the determination of mercury, due to its simplicity, because of the relatively low cost of operation, high sensitivity (ng mL^{-1}), and selectivity.[27,28] Hg(II) ions are reduced to Hg(0) in the acidic medium with $NaBH_4$. The mercury vapors generated during the process are transported by a carrier gas (Ar) to the atom cell located in the path of the hollow cathode lamp. Mercury is monitored at 253.7 nm.

5. Conclusions

In this study, we focused on semiconductor materials that remove trace toxic metals from water. SiO_2@CeO_2 CSNs were synthesized, using chemical precipitation, and investigated as adsorbents for the removal of Hg(II) from water successfully. In addition, it was seen that all particles were spherical from SEM and TEM analyses. Adsorption capacity was increased by increasing the pH value due to electrostatic attraction but was decreased by temperature. Our results showed that 81.2% removal of Hg(II) is possible at optimal conditions (pH 8, 1.0 mg L^{-1}, and amount of adsorbent: 0.05 g). As a result, it was seen that CSNs can be utilized in water purification systems and can remove Hg(II) as well as other heavy and toxic metals.

References

1. Hadavifar, M.; Bahramifar, N.; Younesi, H.; Li. Q. *Chem. Eng. J.* **2014**, 237, 217-228.
2. Inbaraj, B. S.; Sulochana, N. *J. Hazard. Mater.* **2006**, *133*, 283-290.
3. Clarkson, T. W. *Environ. Health. Perspect.* **1992**, *100*, 31-38.
4. Tuzcu, E. T.; Atalay, M. U. *Turk. J. Eng. Environ. Sci.* **2011**, *35*, 93-105.
5. Bazrafshan, E.; Mohammadi, L.; Moghaddam, A. A.; Mahvi, A. H. *J. Environ. Health Sci. Eng.* **2015**, *13*, 74-90.
6. Hunsom, M.; Pruksathorn, K.; Damronglered, S.; Vergnes, H.; Duverneuil, P. *Water Res.* **2005**, *39*, 610-616.
7. Chung, S. H.; Lee, D. W.; Kim, M. S.; Lee, K. *J. Colloid Interface Sci.* **2011**, *355*, 70-75.
8. Li, B.; Wei, X.; Pan, W. *J. Power Sources* **2009**, *193*, 598-601.
9. Marzaán, L. M.; Giersig, M.; Mulvaney, P. *Langmuir* **1996**, *12*, 4329-4335.
10. Ocana, M.; Adres-Verges, M.; Pozas, R.; Serna, C. J. *J. Colloid Interface Sci.* **2006**, *294*, 355-361.
11. Zhai, Y.; Zhang, S; Pan, H. *Mater. Lett.* **2007**, *61*, 1863-1866.
12. Zhu, B.; Luo, Z. *Mater. Res. Bull.* **1999**, *34*, 1507-1512.
13. Song, X.; Jiang, N.; Li, Y.; Xu, D.; Qiu, G. *Mat. Chem. Phys.* **2008**, *110*, 128-135.
14. Uğurlu, M.; Kula, İ.; Karaoğlu, M. H.; Arslan Y. *Environ. Sci. Pollut. Res.* **2009**, *28*, 547-557.
15. Yadava, K. P.; Tyagi, B. S.; Singh, V. N. *J. Chem. Technol. Biotechnol.* **1991**, *51*, 47-60.
16. Blazquez, G.; Hernainz, F.; Calero, M.; Ruiz-Nunez, M. L. F. *Process Biochem.* **2005**, *40*, 2649-2654.
17. Hakami, O.; Zhang, Y.; Banks, C. J. *Water Res.* **2012**, *46*, 3913-3922.
18. Erdem, M.; Yuksel, E.; Tay, T.; Cimen, Y.; Turk, H. *J. Colloid Interface Sci.* **2009**, *333*, 40-48.
19. Zhou, L.; Liu, Z.; Liu, J.; Huang, Q. *Desalination* **2010**, *258*, 41-47.
20. Karaoglu, M. H.; Kula, İ.; Uğurlu, M. *Clean* **2013**, *41*, 548-556.
21. Raji, F.; Pakizeh, M. *Appl. Surf. Sci.* **2013**, *282*, 415-424.
22. Turan, P.; Dogan, M.; Alkan M. *J. Hazard. Mater.* **2007**, *148*, 56-63.
23. Lohania, M. B.; Singh, A.; Rupainwar, D. C.; Dhar, D. N. *J. Hazard. Mater.* **2008**, *159*, 626-629.
24. Mou, F.; Guan, J.; Xiao, Z.; Sun, Z.; Shi, W.; Fan, X. *J. Mater. Chem.* **2011**, *21*, 5414-5421.
25. Arshadi, M.; Gholtash, J. E.; Zandiand, H.; Foroughifard, S. *RSC Adv.* **2015**, *5*, 43290-43302.
26. Jaerger S.; Santos A.; Fernandes, A. N.; Almeida, C. A. P. *Water Air Soil Pollut.* **2015**, *226*, 236-241.
27. Tewari B. B.; Mohan, D.; Kamaluddin, A. *Colloid Surface A.* **1998**, *131*, 89-93.
28. Sirry, S.; Soltan M. E. *Chem. Ecol.* **2004**, *20*, 449-458.